



Five Mirror System Derived from the Numerical Solutions of All Zero 3rd-Order Aberrations and Zero 5th-Order Spherical Aberration for Deep-Ultraviolet Optical Lithography

Dong Hee LEE, Hong Jin KONG and Sang Soo LEE

Department of Physics, Korea Advanced Institute of Science and Technology,
373-1 Kusong-dong, Yusong-gu, Taejon, 305-701, Seoul Korea

(Received August 2, 1993; Accepted December 1, 1993)

A five mirror system with a reduction magnification ($M=+1/5$) is designed for deep-UV optical lithography. Initially, numerical solutions of all zero 3rd-order aberrations and zero 5th-order spherical aberration are obtained for the spherical mirror system. Next, by the optimization method, the aspherization is carried out to the two spherical mirrors to obtain a system that has as less residual aberrations, higher NA and improved MTF as possible. We have finally obtained the system of which NA is 0.45, the depth of focus is $0.8\ \mu\text{m}$ and the resolution is about 600 cycles/mm at the 50% MTF value criterion for the coherence factor $\sigma=1.0$ and $\lambda=193\ \text{nm}$ (ArF excimer laser line).

1. Introduction

There is a growing trend that the optical systems for the submicron lithography have larger numerical aperture (NA) and use shorter wavelengths in order to realize the higher resolution.¹⁻⁴⁾ However, in the refractive optical systems, there are a number of difficulties in following this trend. Especially at the wavelength 248 nm of the KrF excimer laser beam or the wavelength 193 nm of the ArF excimer laser beam, the light absorption in the optical refractive materials and the chromatic aberration due to the broad linewidths are troublesome problems. Those difficulties may be overcome in the all-reflective mirror system. The Dyson series consist of two elements which are a refractive lens and a reflective mirror in that both curved surfaces are concentric. Because these systems (magnification $M=-1$) use the characteristics of two concentric surfaces, all third-order and some higher-order aberrations are eliminated, and therefore they have the considerably large NA (0.5-0.7) but their shortcomings are in the chromatic aberrations and lack of the reduction capability.⁵⁻⁷⁾ Then, in 1975, as a fully reflective system, Offner proposed a concentric two-spherical mirror system with three reflections in that all third-order aberrations are eliminated.⁸⁾ But the

shortcoming of this system is again in the fixed magnification ($M=-1$). Meanwhile, as the fully reflective system with a controllable magnification, the four-mirror system composed of a Cassegrainian and an inverse Cassegrainian configurations with a reduction magnification ($M=+1/5$) was reported.⁹⁾ They started with the compact forms of the Gaussian bracket expressions of the aberrations and, from the numerical solutions which give zero in four aberrations out of five third-order aberrations, they obtained the spherical mirror system. It was finally optimized and aspherized to minimize the residual aberrations and to have good NA. This system had two design parameters remaining free; however, its NA was limited at 0.38. In order to make a breakthrough we propose in this paper a five mirror system. By increasing the number of surfaces to five, we could obtain numerical solutions which give all zero third-order aberrations and zero fifth-order spherical aberration and still keep two design parameters remaining free. With these two design parameters (d_0 and d_1 in **Fig. 1(a)**), we have obtained the solution domain on the d_0 - d_1 plane. By the optimization on curvatures and asphericities of two mirrors (c_4 and c_5 in **Fig. 1(a)**) of any system in the solution domain, we have found that their depth of focus obtained from the de-

focused spot diagrams is about $0.8 \mu\text{m}$ and their NA is larger than 0.40 for the ArF excimer laser line. We have then considered the size of the mirrors, the amount of the residual aberrations, the illumination uniformity of the systems, the telecentricity, the obscuration in the 1st mirror by the 2nd mirror and the MTF curve. From these considerations, we have finally obtained the system whose NA is 0.45, image field diameter is 5.2 mm, depth of focus is $0.8 \mu\text{m}$ and resolution is about 600 cycles/mm (i.e. half the grating constant; $0.8 \mu\text{m}$) at the 50% MTF value criterion¹⁰⁾ for the coherence factor $\sigma=1.0$ ^{11,12)} and $\lambda=193 \text{ nm}$ (ArF excimer laser line).

2. Analyses of the Aberration Conditions for the Five Mirror System to Be Free from All 3rd-Order Aberrations and 5th-Order Spherical Aberration

The schematic diagram of the five mirror system is shown in Fig. 1(a). In this system, the aperture stop lies on the fourth mirror (c_4 in

Fig. 1(a)) and the principal ray makes angle β with the optical axis at the stop. We want the solutions which are free from all third-order aberrations (of which coefficients are S_i , $i=I, II, III, IV$ and V) and the fifth-order spherical aberration (of which coefficient is T_I)¹³⁻¹⁵⁾ for the magnification of $+1/5$. These coefficients of the third-order and fifth-order aberrations were derived and reported by Matsui.¹³⁾ The analytic expressions of the coefficients of fifth-order aberrations were also derived by Buchdahl¹⁴⁾; however, Matsui's expressions are more compact. Therefore, we use his expressions, then those conditions mentioned above are expressed by using the Gaussian brackets []^{16,17)} as follows:

$$S_I = 2u_0^4 \sum_{i=1}^5 (-1)^i c_i g^{2i-1} a_i^2 = \sum_{i=1}^5 I_i = 0, \quad (1)$$

$$S_{II} = 2u_0^3 \beta \sum_{i=1}^5 (-1)^i c_i g^{2i-1} a_i b_i = \sum_{i=1}^5 J_i = 0, \quad (2)$$

$$S_{III} = 2u_0^2 \beta^2 \sum_{i=1}^5 (-1)^i c_i g^{2i-1} b_i^2 = 0, \quad (3)$$

$$S_{IV} = 2u_0^2 \beta^2 \sum_{i=1}^5 (-1)^i [c_i g^{2i-1} b_i^2 - c_i g^7] = 0, \quad (4)$$

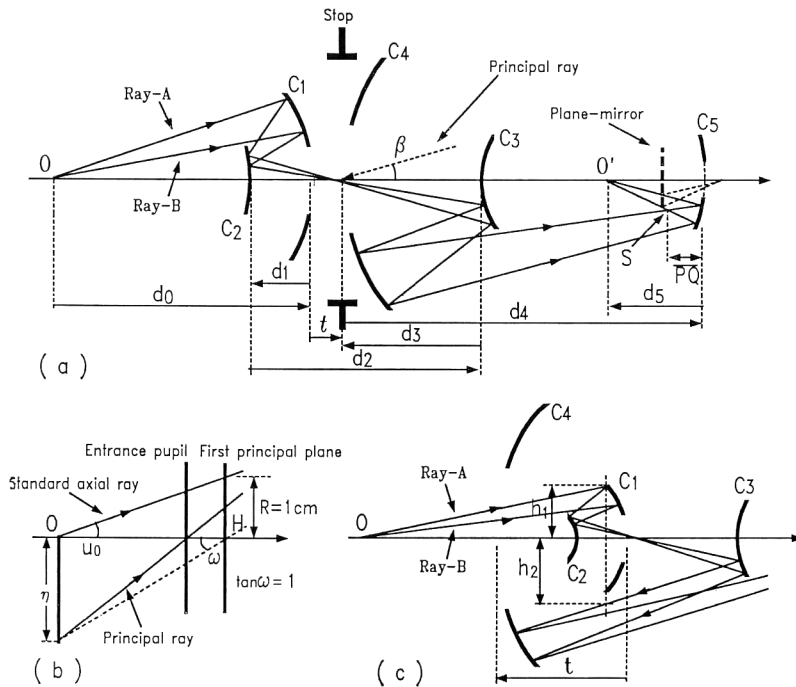


Fig. 1 (a) Typical configuration of a five spherical mirror system with the stop at the vertex of the fourth mirror surface. (b) Required conditions of the initial marginal ray and the initial principal ray for the calculation of coefficients of aberrations.^{13,15)} (c) In case of $t < 0$, the relation between h_1 and h_2 . Ray-A, Ray-B: the rays from the axial object point through the full margin of the entrance pupil and through the 0.7 margin of the entrance pupil, respectively.

$$S_V = 2u_o\beta^8 \sum_{i=1}^5 (-1)^i [c_i g_{2i-1} b_i^3 / a_i - c_i g_i^3 b_i / a_i] = 0, \quad (5)$$

$$T_I = \sum_{i=1}^5 (T_i + 6I_i \sum_{k=1}^{i-1} V_k - 6J_i \sum_{k=1}^{i-1} I_k) = 0, \quad (6)$$

$$M = 1/g_{10} = 1/5, \quad (7)$$

where,

$$\begin{aligned} V_i &= -2(-1)^i u_o^2 c_i g_{2i-1} a_i (1 + u_o \beta a_i e_i), \\ T_i &= -6u_o^6 c_i^2 g_{2i-1} a_i^2 [2a_i + 2g_{2i-2} - (-1)^i c_i g_{2i-1}], \\ u_o &= -\frac{[2c_1, -d_1, -2c_2, d_2, 2c_3, -d_3, -2c_4, d_4, 2c_5]}{g_{10} + 1}, \end{aligned} \quad (8)$$

$$\beta = \frac{1}{g_7 u_o}, \quad (9)$$

$$\begin{aligned} g_0 &= 1, \\ g_1 &= [d_0], \\ g_2 &= [d_0, 2c_1], \\ g_3 &= [d_0, 2c_1, -d_1], \\ g_4 &= [d_0, 2c_1, -d_1, -2c_2], \\ g_5 &= [d_0, 2c_1, -d_1, -2c_2, d_2], \\ g_6 &= [d_0, 2c_1, -d_1, -2c_2, d_2, 2c_3], \\ g_7 &= [d_0, 2c_1, -d_1, -2c_2, d_2, 2c_3, -d_3], \\ g_8 &= [d_0, 2c_1, -d_1, -2c_2, d_2, 2c_3, -d_3, -2c_4], \\ g_9 &= [d_0, 2c_1, -d_1, -2c_2, d_2, 2c_3, -d_3, -2c_4, d_4], \\ g_{10} &= [d_0, 2c_1, -d_1, -2c_2, d_2, 2c_3, -d_3, -2c_4, d_4, 2c_5], \\ a_1 &= [d_0, c_1], \\ a_2 &= [d_0, 2c_1, -d_1, -c_2], \\ a_3 &= [d_0, 2c_1, -d_1, -2c_2, d_2, c_3], \\ a_4 &= [d_0, 2c_1, -d_1, -2c_2, d_2, 2c_3, -d_3, -c_4], \\ a_5 &= [d_0, 2c_1, -d_1, -2c_2, d_2, 2c_3, -d_3, -2c_4, d_4, c_5], \\ b_1 &= [c_1, -d_1, -2c_2, d_2, 2c_3, -d_3], \\ b_2 &= [-c_2, d_2, 2c_3, -d_3], \\ b_3 &= [c_3, -d_3], \\ b_4 &= 1, \\ b_5 &= [d_4, c_5], \\ e_1 &= [-d_1, -2c_2, d_2, 2c_3, -d_3], \\ e_2 &= [d_2, 2c_3, -d_3], \\ e_3 &= [-d_3], \\ e_4 &= 0, \\ e_5 &= [-d_4]. \end{aligned}$$

In these equations, c_i ($i=1, 2, 3, 4$ and 5) is the curvature of each mirror, d_i ($i=0, 1, 2, 3$ and 4) is the distance between mirrors (Fig. 1(a)), u_o in Eq. (8) is the initial paraxial angle of the ray from the axial object point passing at the height of 1 (i.e. in Fig. 1(b), $R=1$ cm) on the 1st principal plane,^{13,15)} and β in Eq. (9) is the angle, at the stop, made by the principal ray which leaves the object at the height η defined by the condition that the tangent of the object half-field angle ($\tan \omega = (\eta/OH)$), viewed from the 1st principal point, is 1 as shown in Fig. 1(b).^{13,15)} These conditions for u_o and β derived

from the conditions, $R=1$ cm and $\tan \omega=1$, shown in Fig. 1(b) are needed to obtain the coefficients of aberrations.^{13,15)} The Helmholtz-Lagrange invariant is then -1 .

From Eq. (4), which shows the Petzval sum is zero, we obtain that

$$c_5 = -c_1 + c_2 - c_3 + c_4. \quad (10)$$

And, after some manipulation, we find Eq. (7) to give the expression for d_4 , which is

$$d_4 = \frac{M^{-1} - 2c_5 g_7 - g_8}{2c_5 g_8}. \quad (11)$$

Therefore, the wanted five mirror system should satisfy the Eqs. (1), (2), (3), (5), (6), (10) and (11) simultaneously.

3. Numerical Method and the Domain of Solutions for Spherical Mirror System

As mentioned in the previous section we have ten design parameters for a five spherical mirror system, but to satisfy the condition of all zero third-order aberrations and zero fifth-order spherical aberration and to satisfy the magnification condition ($M=+1/5$), we lose seven degrees of freedom. In addition, by setting $c_1=-1$ for scaling of the system, there are finally two parameters remaining free, which are d_0 and d_1 in this work. The minus sign for c_1 indicates the front two-mirror system is either Cassegrainian or Gregorian. For appropriately given values of d_0 and d_1 , the simultaneous equations (Eqs. (1), (2), (3), (5), (6), (10) and (11)) are solved by computer calculations which are programmed by using the optimization method.¹⁶⁾ The flow chart of this program is shown in Fig. 2. By the repetitive application of this procedure for the appropriate range of d_0 and d_1 , we can find the numerical solutions and the solution domain. However, in order to obtain realistic systems, we ought to impose several additional conditions; $d_1 < 0$, $d_3 < 0$, $d_2 > 0$, $d_4 > |d_3|$, $vig_1 < 0.7$, $vig_2 < 0.7$, where vig_1 is the central obscuration in the 1st mirror by the 2nd mirror, vig_2 is that in the 4th mirror by the 3rd mirror. We note that $(vig_i)^2 \times 100\%$ ($i=1, 2$) of the rays from the axial object point is obscured. Also, in order that the image plane is at the right hand side of c_5 by placing a plane-mirror as shown in Fig. 1(a), we ought to impose the conditions of $2 \times \overline{PQ} < |d_5|$ and $\overline{PQ} < d_4 + d_3$, where \overline{PQ} is the distance from S to c_5 in Fig. 1(a), S being the crossing point of Ray-A (which is the ray from the axial object point passing at the full margin of the entrance pupil) and Ray-B (which is the ray from the axial

object point passing at the 0.7 margin of the entrance pupil) in the space between c_3 and c_5 . Further, in case that the thickness t , which is equal to $d_1+d_2+d_3$, is negative, the rays from the 3rd to the 4th mirror, are not to be obscured by the 1st mirror, so that we also impose the condition of $h_1 < h_2$, where h_1 is the incident height of Ray-A at the margin of c_1 and h_2 is the incident height of Ray-B which may pass the third mirror to the fourth mirror as seen in Fig. 1(c). The results thus obtained are shown in Fig. 3. Figure 3(a) is the solution domain diagram in which the wanted five mirror systems can exist for $c_1 = -1$ and $NA = 0.4$. The front

four mirrors of any five mirror system in this domain make the Cassegrainian-inverse Cassegrainian configuration. Figure 3(b) shows the contour map of the residual transverse spherical aberration calculated for NA of 0.4 and the effective focal length of -100 mm. The range of the residual spherical aberration as shown in the figure

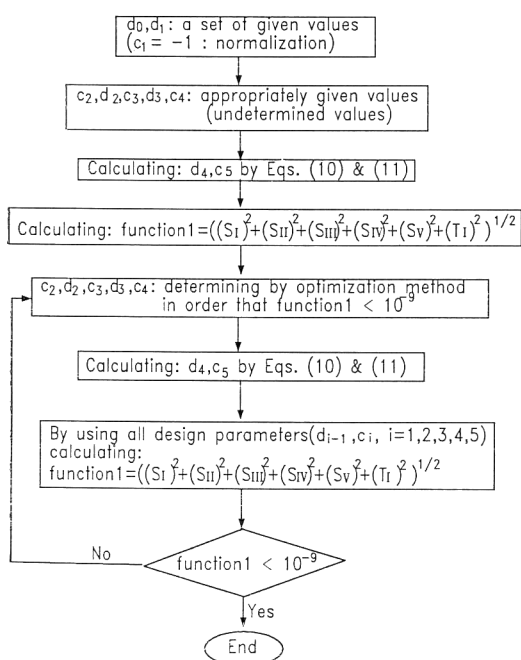


Fig. 2 The flow chart for solving the simultaneous equations of five spherical mirror systems.

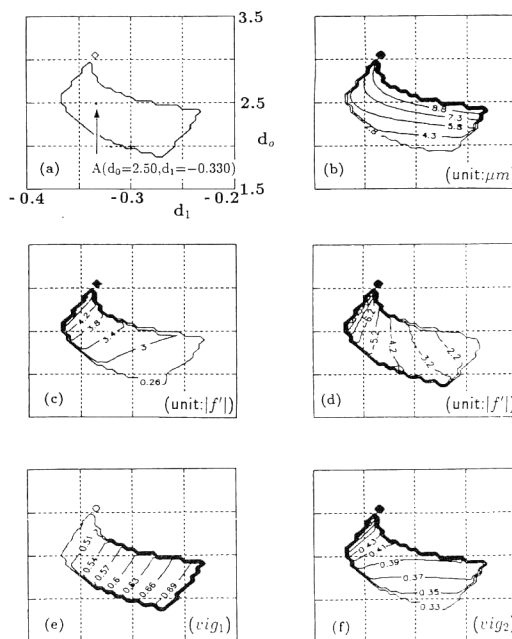


Fig. 3 Solution domain and various characteristics of the five spherical mirror systems (NA = 0.40) which are free from all third-order aberrations and fifth-order spherical aberration (y-axis: d_0 , x-axis: d_1). (a) solution domain, (b) contour map of the residual transverse spherical aberration, (c) contour map of size of the largest mirror, (d) contour map of the thickness t from c_1 to c_4 , (e) contour map of vig_1 and (f) contour map of vig_2 .

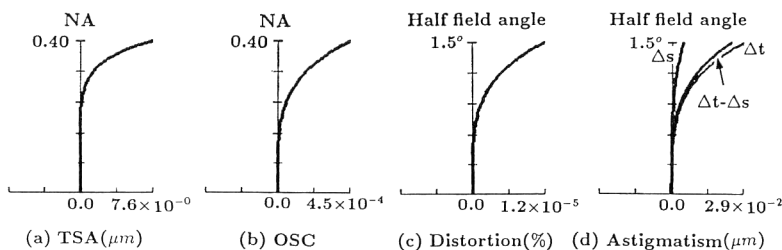


Fig. 4 (a), (b), (c) and (d) are the residual finite ray aberrations for the five spherical mirror system A in Fig. 3(a) with focal length of -100 mm and object-field-size of 26 mm for ArF excimer laser beam. TSA : transverse spherical aberration ; OSC : offense against sine condition ; Δt : tangential ray aberration ; Δs : sagittal ray aberration, and astigmatism : $\Delta t - \Delta s$.

is about $2.8 \mu\text{m}$ to $9.6 \mu\text{m}$. Figure 3(c) reveals the contour map of the radius of the largest mirror in the unit of the absolute value of focal length ($|f'|$). The range of the radii is about 2.6 times to 5.1 times. Figure 3(d) shows the contour map of the thickness $t(=d_1+d_2+d_3)$ in the unit of the absolute value of focal length. The range of t is about -1 times to -9 times of $|f'|$. Figure 3(e) reveals the contour map of the values of viq_1 . The range of the value is about 0.71 to 0.48. Figure 3(f) reveals the contour map of the values of viq_2 and the range of the value is about 0.33 to 0.52. **Figure 4** shows the residual finite ray aberrations of a initial solution located at A ($d_0=2.50$, $d_1=-0.330$) in the solution domain diagram of Fig. 3(a) (NA, 0.4; f' , -100 mm; object-field-size, 26 mm). The final system described in the next section is the outcome of the solution at A shown in Fig. 3(a). Although the third- and fifth-order spherical aberrations have been eliminated completely, the residual spherical aberration still remains as much as $7.6 \mu\text{m}$ due to the seventh- and higher-order aberrations [Fig. 4(a)]. Also, the residual coma, which is composed of the higher-order aberrations, represented by OSC in Fig. 4(b), is still quite large. However, the distortion of the system is about 3 \AA in the full-field [Fig. 4(c)], which is small enough to satisfy the requirement of the submicron lithographic optics,^{19,20)} and the astigmatism of the system is about $0.03 \mu\text{m}$ in the full-field [Fig. 4(d)], which is again small enough. These tendencies, i.e. spherical aberration is of the order of μm , OSC is of the order of 10^{-4} and distortion and astigmatism are well corrected, are the characteristics common to all solutions within the domain shown in Fig. 3

(a). Therefore, for the five mirror system to have higher NA, it is necessary to correct the residual spherical aberration and the residual coma. This could be accomplished by the aspherization of the last two surfaces of the five mirror system.

4. Correction of Residual Aberrations by Aspherization, Telecentricity and the Final System

An aspheric surface is represented by

$$z = \frac{cy^2}{1 + (1 - c^2y^2)^{1/2}} + a_4y^4 + a_6y^6 + a_8y^8 + a_{10}y^{10}, \quad (12)$$

where c is the curvature of the surface, a_i ($i=4, 6, 8, 10$) is the coefficient of departure from the base sphere and y is the marginal ray height at the surface. We add these asphericities to the fourth and fifth spherical mirrors, and optimize the system by the simple damped least squares method.¹⁸⁾ In the optimization process, the aspherization of the fourth mirror is used mainly to correct the residual spherical aberration. It is well known that the aspherization of the surface, where the iris stop is placed, has efficient influence on the spherical aberration. And the aspherization of the fifth mirror is used mainly to correct the residual coma. Judging from the defocused spot diagrams, most solutions in the solution domain shown in Fig. 3(a) give the systems with the depth of focus larger than $0.8 \mu\text{m}$, the object-field-size of 26 mm and NA higher than 0.40 that give the spot diagrams of which radius is less than or equal to the Rayleigh radius of $0.29 \mu\text{m}$ for 193 nm of the ArF excimer laser beam. It is desirable that the relative amount of light (100% for the axial ray) from any point on the object field passing through the system is over 80% and,

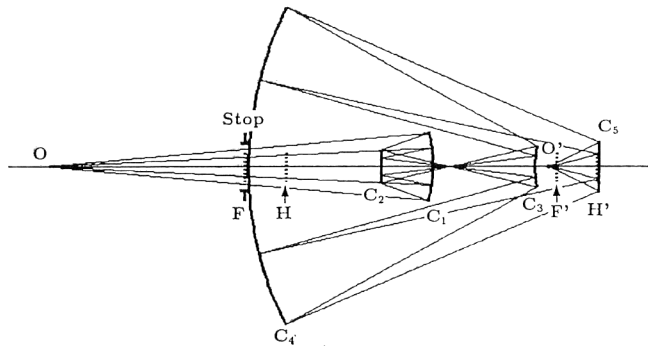


Fig. 5 Configuration of the aspherized five mirror system (c_4, c_5 are aspherical). The stop of the system lies on the first focal plane. F, F': 1st and 2nd focal plane, H, H': 1st and 2nd principal plane.

at the same time, the residual aberrations are as small as possible. But, because the obscuration in the 1st mirror by the 2nd mirror has definite influence on the MTF curve of the system, it is more desirable that the viq_1 is as small as possible. Then the viq_2 is less than the viq_1 as shown in Fig. 3(e) and (f), so that the effect of the viq_2 on the MTF is not necessary. These required conditions are fulfilled by the aspherization of the solution at A in Fig. 3(a). Finally, the system must be telecentric in the image space. The aperture stop of the system is then moved to the 1st focal plane. In **Fig. 5**, the final configuration of the aspherized five mirror system and the ray paths through the system for axial rays (a full-marginal ray and a 0.55-marginal ray) are shown. The design data of this system before the aspherization and after the aspherization are listed in **Tables 1** and **2**, and the clear apertures and the hole diameters of the mirrors of the system are listed in **Table 3**. In **Fig. 6**, the residual finite ray aberrations of the system are illustrated. The spherical aberration is in the order of $10^{-2} \mu\text{m}$ [Fig. 6(a)] and the numerical aperture of this

system is 0.45, which gives the Rayleigh radius of $0.26 \mu\text{m}$ for 193 nm of the ArF excimer laser beam. And the field angle is 3 deg. which is equal to object-field-diameter of 26 mm for the focal length of -100 mm . The distortion of this system is only about 0.6 \AA in the full-field [Fig. 6(c)]. The direction cosine of the principal ray to the optical axis (z -axis) in the image space is less than 2×10^{-5} [Fig. 6(e)], so the system is sufficiently telecentric. Figure 6(f) illustrates the relative amount of light passing through the system over the field (i.e. the illumination uniformity is shown). It is about 84.5% for the full-field. **Figure 7** shows spot diagrams for three field angles and five defocused image positions. This shows that most of the rays fall within a $0.26 \mu\text{m}$ -Rayleigh-radius circle over a full-field, with the depth of focus of $0.8 \mu\text{m}$ (δz ; $-0.4 \mu\text{m}$ to $+0.4 \mu\text{m}$, ref. to Fig. 7). In this figure, the circles denote the Airy disk (radius; $0.26 \mu\text{m}$) for the ArF excimer laser beam ($\lambda = 0.193 \mu\text{m}$). The MTF values for this aspherized five mirror system are depicted in **Fig. 8** and **Fig. 9**. Figure 8 shows that the system have the resolution of

Table 1 Initial spherical mirror design data before aspherization of the five spherical mirror system corresponding to the point A in Fig. 3(a), which is free from all third-order aberrations and fifth-order spherical aberration with stop at the vertex of fourth mirror surface ($f' = -10 \text{ cm}$).

| | Object | C_1 | C_2 | C_3 | C_4 | C_5 |
|--------------------------------|-----------|------------|------------|------------|-----------|------------|
| Curvature (cm^{-1}) | | -0.0259042 | -0.0151021 | 0.0266295 | 0.0111224 | -0.0047050 |
| Distance (cm) | 96.509463 | -12.739249 | 38.029636 | -71.023939 | 86.842304 | |

Table 2 Design data of the aspherized five mirror system for ArF excimer laser line ($f' = -10 \text{ cm}$).

| | Object | Stop | C_1 | C_2 | C_3 | C_4 | C_5 |
|--------------------------------|-------------------------|-----------|----------------------------|-----------------------------|-----------------------------|-------------------------------|------------|
| Curvature (cm^{-1}) | | | -0.0259038 | -0.0151018 | 0.0266291 | 0.0111254 | -0.0047008 |
| Distance (cm) | 50.000000 | 46.511008 | -12.739453 | 38.030245 | -71.025076 | 86.843604 | |
| | Aspherical coefficients | | | | | | |
| | | | a_4 (cm^{-3}) | a_6 (cm^{-5}) | a_8 (cm^{-7}) | a_{10} (cm^{-9}) | |
| Fourth surface | | | 1.623994×10^{-11} | $-3.660871 \times 10^{-14}$ | $-8.247089 \times 10^{-18}$ | $-6.803292 \times 10^{-21}$ | |
| Fifth surface | | | -1.367644×10^{-8} | -4.319612×10^{-9} | 2.892166×10^{-11} | $-1.092991 \times 10^{-18}$ | |

Table 3 Diameters of clear apertures and holes of the mirrors for the system given by Table 2 (unit : cm).

| | Stop | C_1 | C_2 | C_3 | C_4 | C_5 |
|----------------|------|-------|-------|-------|-------|-------|
| Clear aperture | 9.04 | 17.27 | 8.29 | 10.64 | 79.60 | 13.07 |
| Hole diameter | 0.00 | 8.29 | 0.00 | 0.00 | 17.27 | 0.00 |

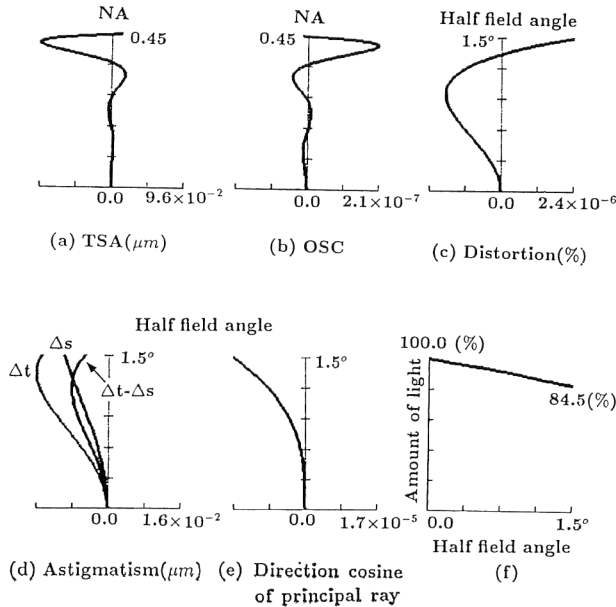


Fig. 6 (a), (b), (c) and (d) are the residual finite ray aberrations of the aspherized five mirror system with focal length of -100 mm, object-field-size of 26 mm and NA of 0.45 for ArF excimer laser beam, (e) is the direction cosine of principal ray in the image space, and (f) is the relative amount of light passing through the system, TSA : transverse spherical aberration; OSC : offense against sine condition; Δt : tangential ray aberration; Δs : sagittal ray aberration, and astigmatism : $\Delta t - \Delta s$.

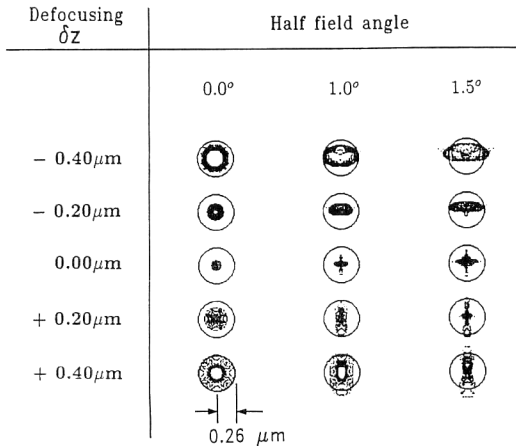


Fig. 7 Spot diagrams of the aspherized five mirror system for three half field angles at five defocused image positions. The depicted circle is the Airy disk (radius $R=0.26\mu\text{m}$) for ArF excimer laser beam.

about 600 cycles/mm (i.e. half the grating constant ; $0.8\mu\text{m}$) at the 50% MTF value criterion¹⁰⁾ for the coherence factor $\sigma=1.0$ and the depth of focus of $0.8\mu\text{m}$, the diffraction-limited perfor-

mance is achieved for the 0.0° field and the maximum resolution is about 850 cycles/mm. Figure 9 shows the theoretical MTF values of the 0.0° field and 1.5° field images for the partial coherent illumination cases (i.e. $\sigma=0.7, 0.8, 0.9$ and 1.0). In this figure we see that at the 0.0° field the higher the coherence factor is, the lower the resolution is, for the 50% MTF value criterion.

5. Conclusion

A five spherical mirror system with a magnification of $+1/5$ has been obtained from the condition of all zero 3rd-order aberrations and zero 5th-order spherical aberration. It is selected from the two-dimensional distribution of the solutions for the five spherical mirror system which are represented on the d_0-d_1 plane. By the aspherization of the last two mirrors by means of the optimization technique for finite ray aberrations and shifting the stop to the first focal plane, we have obtained the system with minimal residual aberrations, the largest possible NA and sufficient telecentricity in the image space. For the focal

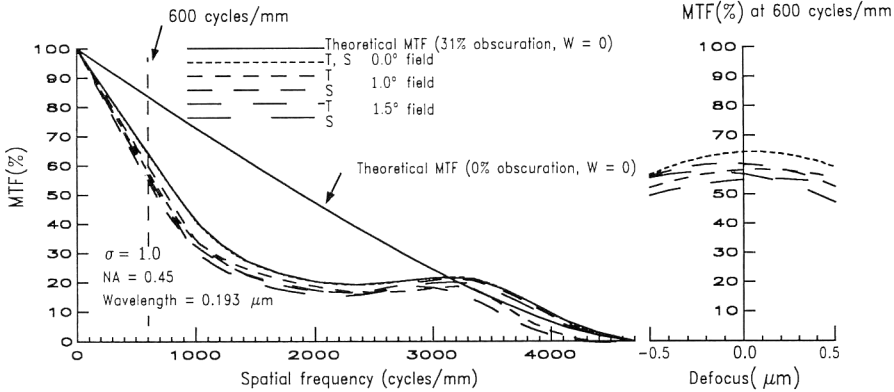


Fig. 8 MTF through frequency (cycles/mm) and through focus of the aspherized five mirror system for three half field angles at the Gaussian image position in case of the coherence factor $\sigma=1.0$. W : residual aberration.

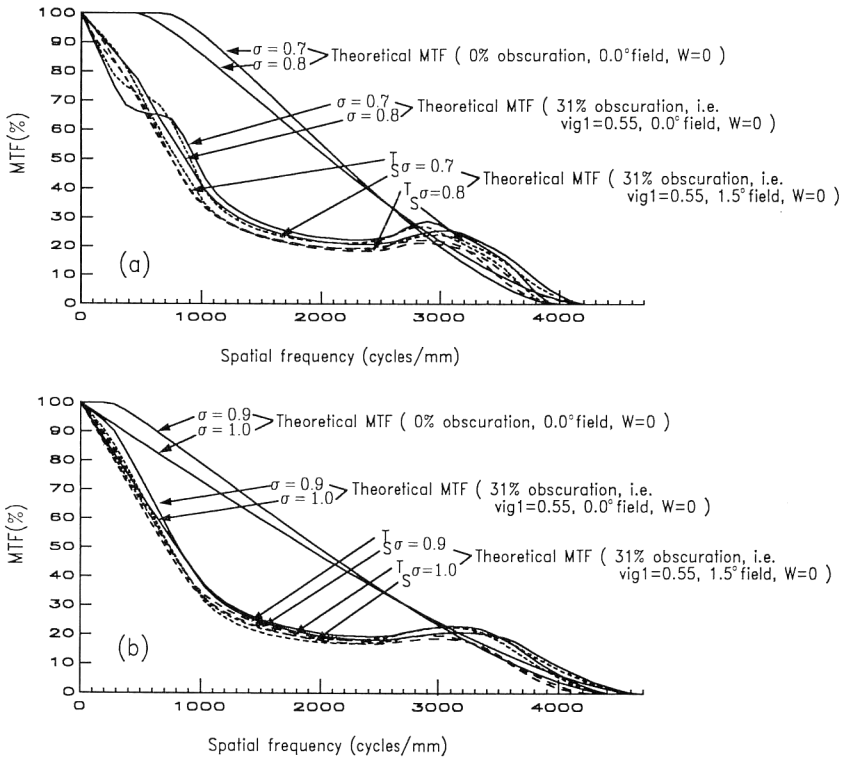


Fig. 9 Theoretical MTF of the aspherized five mirror system for the 0.0° field and 1.5° field images at the Gaussian image position in cases of the various partial coherent illuminations (i.e. $\sigma=0.7, 0.8, 0.9$ and 1.0). W : residual aberration; T : tangential MTF; S : sagittal MTF.

length of -100 mm, the final system has NA of 0.45 , the depth of focus of $0.8 \mu\text{m}$, the image-field-diameter of 5.2 mm and the resolution of about 600 cycles/mm at the 50% MTF value criterion for the coherence factor $\sigma=1.0$ and $\lambda=193$ nm (ArF excimer laser line). As the selected

five spherical mirror system before the aspherization has small initial residual aberrations, we could reach to the final aspherized system faster obtaining the higher NA and resolution than the previously reported four mirror system.⁹⁾ The system uses, however, the clear aperture of nearly

80 cm in diameter, so that we are trying to improve the design by finding solutions which give shorter diameters of the clear apertures. Also, we are interested in the soft X-ray lithography optics and trying to develop an efficient reflective projection system from the one such as reported in this paper.^{21,22)}

Acknowledgements

We thank J. U. Lee of the Cheongju University, S. C. Park of the Gold Star Co., Ltd., and J. T. Kim of the Korea Advanced Institute of Science and Technology for the kind discussions. Their previous works carried out in this laboratory have been useful throughout the present work.

References

- 1) H.L. Stover: "Lens specifications and distortions," *Optical Microlithography VI, Proc. SPIE 772*, ed. H.L. Stover (1987) pp. 2-4.
- 2) G.E. Fuller: "Optical lithography status," *Solid State Technol.*, **30**, 9 (1987) 113-118.
- 3) J.H. Bruning: "Lithographic lenses for microcircuit fabrication," *Opt. News*, **13**, 6 (1988) 23-24.
- 4) S. Okazaki: "Lithographic technology for future ULSIs," *Solid State Technol.*, **34**, 11 (1991) 77-82.
- 5) J. Dyson: "Unit magnification optical system without seidel aberrations," *J. Opt. Soc. Am.*, **49** (1959) 713-716.
- 6) R.M.H. New, G. Owen and R.F.W. Pease: "Analytic optimization of Dyson optics," *Appl. Opt.*, **31** (1992) 1444-1449.
- 7) A. Grenville, R.L. Hsieh, R. von Bunau, Y.-H. Lee, D.A. Markle, G. Owen and R.F.W. Pease: "Markle-Dyson optics for 0.25 μm lithography and beyond," *J. Vac. Sci. Technol. B*, **9** (1991) 3108-3112.
- 8) A. Offner: "New concepts in projection mark aligners," *Opt. Eng.*, **14** (1975) 130-132.
- 9) J.T. Kim, H.J. Kong and S.S. Lee: "Improved four-mirror optical system for deep-ultraviolet submicrometer lithography," *Opt. Eng.*, **32** (1993) 536-541.
- 10) C. Wang and D.L. Shealy: "Differential equation design of finite-conjugate reflective systems," *Appl. Opt.*, **32** (1993) 1179-1188.
- 11) H. Tanabe: "Comparison of super-resolution techniques in the optical system of steppers," *Kogaku*, **21** (1992) 415-423.
- 12) K. Ushida: "Projection optics for optical steppers," *Kogaku*, **20** (1991) 70-75.
- 13) Y. Matsui: *Lens Sekkeiho (The Method of Lens Design, written in Japanese)*, 1st ed. (Kyoritsu Publication Inc., Tokyo, 1972) pp. 77-128.
- 14) H.A. Buchdahl: *Optical Aberration Coefficients*, 1st ed. (Dover Publications Inc., New York, 1968).
- 15) T. Kusakawa: *Lens Kogaku (Lens Optics, written in Japanese)*, 1st ed. (Tokai Univ. Press, Tokyo, 1988) pp. 218-259.
- 16) M. Herzberger: *Modern Geometrical Optics*, 1st ed. (Interscience, New York, 1958) pp. 457-462.
- 17) K. Tanaka: "Paraxial theory in optical design in terms of Gaussian brackets," *Progress in Optics XXII*, ed. E. Wolf (North-Holland, Amsterdam, 1986) pp. 63-111.
- 18) R.W. Daniels: *An Introduction to Numerical Methods and Optimization Techniques*, 1st ed. (North-Holland, New York, 1978) chap. 8.
- 19) B.J. Lin: "The path to subhalf-micrometer optical lithography," *Optical/Laser Microlithography, Proc. SPIE 922*, ed. B.J. Lin (1988) pp. 256-269.
- 20) R. Hirose: "New g-line lens for next generation," *Optical/Laser Microlithography II, Proc. SPIE 1088*, ed. B.J. Lin (1989) pp. 178-186.
- 21) Canon: European Patent No. 87306037.0 (1987).
- 22) V.K. Viswanathan and B.E. Newnam: "Development of reflective optical system for XUV projection lithography," *Soft X-Ray Projection Lithography, Vol. 8 of 1992 OSA Technical Digest Series* (Optical Society of America, Washington, D.C., 1992) pp. 136-137.